Resource Assessment of Large Marine Current Turbine Arrays

D.S. Coles*, L.S. Blunden and A.S. Bahaj
Sustainable Energy Research Group, Energy and Climate Change Division, Faculty of Engineering and the Environment
University of Southampton
Southampton, United Kingdom
* D.coles@soton.ac.uk

***Abstract*— At present, simple analytical and numerical models exist that give approximations for the energy that can be extracted by marine current turbine arrays (MCTAs) from an available resource. This paper first presents an analysis of different methods for conducting a resource assessment to outline the considerations that must be made whilst also identifying areas where more detail is required. Resource assessment using 2-D depth averaged numerical modelling software Telemac-2D is presented to give analysis of the behaviour of the flow in the presence of MCTAs and the effects of array density and seabed roughness on wake length and power generation.**

Keywords—Tidal power, Resource assessment, Rough wall flows, Computational fluid dynamics.

I. Introduction

The deployment of marine current turbines has the potential to generate significant amounts of electricity in different global locations. A key advantage of this technology over other renewable sources of power generation is that the resource is predictable for years to come [1]. This is highly relevant in today's energy market, where there is a demand to generate an increasing amount of electricity in a clean, sustainable and reliable way. Many different turbine designs are being developed with some now installed in different locations around the world. However, for this technology to make a significant contribution towards electricity generation, many devices must be deployed in arrays to make full use of the available resource.

A tidal array will have an impact on the characteristics of the flow around it, which must be considered before installation takes place to ensure there are no detrimental effects such as sediment transport which can destroy the habitat of local wildlife. Therefore, the initial process for deploying MCTAs involves effective resource assessment to ensure power generation can be maximized within the constraints of the environment it is placed in. Doing so will improve investor confidence in the technology which increases the likelihood that capacity will increase around the world in the future.

Many different approaches can be taken for resource assessment and this paper focuses in on some analytical and numerical methods that have been developed in the past. This aims to highlight the important factors that must be considered with respect to array density and seabed roughness, and how these affect power generation and wake length. This is demonstrated with the use of a 2-D numerical model for a simple channel flow.

II. Analysis of Existing Methods for Conducting Resource Assessment

A resource assessment can be simplified by breaking it down into five main tasks [2]:

1. Site selection – Constrained primarily by the average mean cube flow speed, a feature that power generation is highly dependent on, as well as water depth. Dynamics of inertia and bed friction also requires consideration[3].
2. Optimization of turbine sizing – Sizing of turbines to maximise power generation over the life of devices based on the flow characteristics of the resource established in task 1.
3. Optimizing array layout – Power generated by an array is dependent on its layout, due to negative/positive turbine interaction.
4. Quantify the effect of the proposed array on tidal parameters – Use acceptable flow and elevation changes to establish if the proposed array has detrimental effects on its surroundings.
5. Economic viability – Consideration of installation, grid connection, operation and maintenance, decommissioning costs and government incentives to establish financial viability.

Part A of this section addresses task 1 by considering methods for measuring flow velocity to accurately assess the potential for a resource to generate power from a MCTA in its undisturbed state. Focus is then turned to tasks 2 and 3 with respect to how array sizing effects power generation and wake length.

A. Undisturbed State - Site Selection

The most critical feature used to assess a resources' suitability for a MCTA is the mean cube flow velocity, mapped over a tidal cycle. Power dissipation is proportional to

978-0-933957-40-4 ©2013 MTS

velocity cubed, so is highly sensitive to flow velocity, as shown by Equation 1.

$$P = \frac{1}{2} A C_P \rho \upsilon^3 \tag{1}$$

Where P is power (W), A is turbine area (m^2), C_p is power coefficient, ρ is sea water density (kg/m^3) and v is flow velocity (m/s). It is still useful to characterize how velocity changes over time for the purpose of turbine operation, grid requirements and energy storage, especially when all tidal developments around the UK will be exposed to the same spring-neap tidal cycle, but this is out of the scope of this work [4].

Methods for obtaining flow velocity data include the use of Admiralty charts (UKHO) or Acoustic Doppler Current Profilers (ADCPs). Admiralty charts have tidal diamonds which indicate the direction and speed of tidal streams.

Disadvantages of this are that the data are at a low temporal resolution, taken from a short period of measurement and they only give an average flow velocity for the top 10m of the water column, which then relies upon assumptions to be made about the velocity profile of the flow to understand how the flow velocity varies through the whole water column. This can lead to error due to the unpredictable nature of the flow profile. ADCPs can be deployed on the seabed to measure the flow velocity at multiple 'bins' directly above the device in the water column. Alternatively they can be deployed on a vessel that can then scan a large area, or attached to buoys. The main advantages of seabed mounted ADCPs are that they capture the flow profile over a long time period, assuming they remains in the water for long enough, whereas vessel mounted ADCPs are able to scan large areas over relatively short periods of time. ADCPs mounted to buoys can be inaccurate due to near-zero velocities included in averages due to interference from the mooring chain [5].

Flow velocity can vary both in magnitude, as characterized by the mean cube flow velocity, and also in its form throughout the water column, as characterized by its velocity profile. ADCP data from Strangford Lough, Ireland in figure 1 shows how the velocity profile can vary significantly throughout a tidal cycle, and it is not uncommon to see profiles such as 1/10th power laws, which are significantly different from a 1/7th power law that is frequently used to predict energy extraction.

The unpredictable nature of the velocity profile makes power predictions challenging and is a source for error due to the sensitivity of power calculations to flow velocity.

Currently it is envisaged that MCT's will be installed in water of depth of approximately 40 m, assuming a turbine diameter of 10-20m. Results from an ADCP device installed in the Falls of Warness tidal race in Orkney show that in water depths of 45m, wave motion induced significant turbulence in

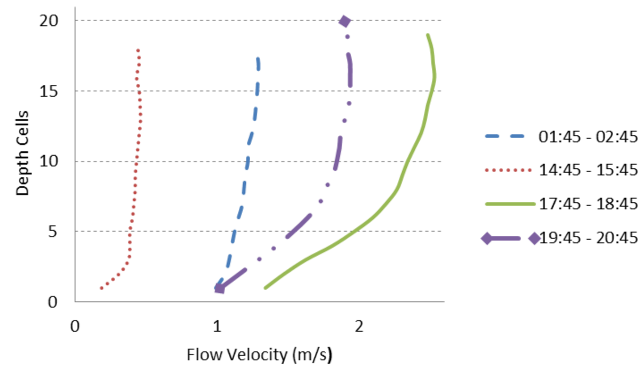

Fig. 1. ADCP data showing the flow speed profile at different times in a tidal cycle. Data source: [UKCMER DTP – Tidal Energy Queen's Marine Laboratory (QML) Portaferry, Northern Ireland, 29th May 2013].

the upper 15m of the water column. Additionally, the sea bed generated turbulence reached up to the center of the water column, therefore the central third of the water column has most suitable conditions for 1st generation MCT devices due to most tranquil conditions and high average flow velocities [6]. Shallower or deeper water becomes unsuitable for 1st generation devices of this size due to installation complications in deeper waters and geometrical and navigational restrictions for shallower water.

B. *Disturbed State*

Once a suitable site has been selected based upon mean cube flow velocity and water depth, optimization of the resource can be considered. This can be approached in several ways:

1. Optimisation of the resource as a whole with no constraints (the upper bound).
2. Optimisation of an array with pre-defined array geometry.
3. Optimisation of an array with a pre-defined installed capacity and array geometry.

Critical to array design is the question, how does power production scale with MCTA size and density? Section C attempts to answer this question by presenting a chronological overview of different methods for predicting power generation that are incorporated in the three approaches above.

C. *Analytical Models*

An upper bound solution to power generation from MCTAs in a simple channel between two large basins has been developed by Garrett and Cummins [3]. This analysis solves the equations of motion in integral form between the two ends of the channel, and concludes the maximum available power to be:

$$P_{\max} = \gamma \rho g a Q_{\max} \tag{2}$$

Where ρ is the density of sea water, g is acceleration due to gravity, a is the amplitude of the sinusoidal height difference between the two ends of the channel and Q_{max} is the maximum volume flux through the channel in its undisturbed state. γ is a coefficient dependent on the phase lag of the current behind the maximum elevation difference in the natural state that varies between 0.21 and 0.24

However, assumptions such as the turbines occupying the whole cross sectional area of the channel and there being no mixing losses in the wakes make Equation 2 an overestimate of the power that can be generated from a resource. Validation using two-dimensional finite element modeling with turbines simulated by increasing drag indicate good comparison with analytical estimates within 10% of numerical results [7].

Detail is added by considering the blockage ratio, ε, defined as the ratio between the total area of the turbines to the cross sectional area of the channel [7]. Bernoulli's equation along with a continuity and momentum balance is used to show that for a given upstream velocity the Lanchester-Betz maximum efficiency factor of 16/27 for a turbine in an infinite medium is increased by a factor of $(1-\varepsilon)^{-2}$, to give:

$$P_{\max} = \frac{16}{27}(1-\varepsilon)^{-2}\frac{1}{2}A\upsilon_0^2 \tag{3}$$

Where ε is the blockage ratio, A is the total turbine rotor area, u_0 is the upstream flow velocity and $0 \le \varepsilon < 1$. This analysis considers only one row of turbines and assumes that the channel cross sectional area remains constant and there is no seabed friction.

The work in this paper considers an array of tidal turbines containing three rows. To express power generation for this scenario, a useful analogy between tidal turbines and wind turbines can be utilized. Assuming the cross sectional area of the turbine is small relative to the area of the channel, the maximum power available can be expressed as the Lanchester-Betz limit:[8]

$$P_{\max} = \frac{8}{27}\rho A\upsilon^3 \tag{4}$$

Where A_T is the total swept area of all turbines in the array and u is the upstream flow velocity. This is an upper bound solution to power generation as it assumes optimum operating conditions in which the flow speed decreases to 2/3^{rds} its upstream magnitude through the turbine and a further 1/3rd as the flow expands in the wake. Furthermore it assumes there is no negative interaction between turbines in the array.

Turbine interaction in a MCTA is in general unknown, making predictions of power potential challenging. Understanding the interaction between rows in an MCTA is key to know how power production scales with array size and density. In reality the wake from a row of turbines can propagate far downstream, so whilst minimizing row interaction is key, eliminating it completely is unrealistic due to spatial limitations. This detail must be accurately incorporated into models for accurate predictions of power generation.

The components of energy extraction from a simple channel flow are examined in detail by Vennell [9]. Energy extraction is broken down into three components by defining a total drag coefficient that contains the contributions from seabed friction, λ_0, drag from support structures, λ_S, and power for electricity production, λ_{prod}:

$$\lambda_{total} = \lambda_0 + \lambda_S + \lambda_{prod} \tag{5}$$

The time averaged total power lost by the flow due to electricity production is given by:

$$\overline{P}_{prod} = 2\lambda_{prod}\left[U_0\left(\lambda_{total}\right)\right]^3 \tag{6}$$

Here Vennell states that the potential for a MCTA to extract energy in a shallow channel is strongly related to where it lies on the P_{drag} curve in relation to its peak. Shallow channels are already highly stressed by seabed friction so have already surpassed their peak, hence they suffer a diminishing return when more turbines are added to fill the cross section.

III. 2-D DEPTH-AVERAGED NUMERICAL MODELS

2-D depth averaged numerical models provide a method for simulating flow computationally that can be validated using real data from ADCPs flow measurements. An advantage of 2-D depth averaged models over 3-D models is computational efficiency, allowing large areas to be modeled without using lots of computing power. This is important, especially around the UK because the continental shelf must be included in the model to incorporate the effect it has in dissipating long waves from the deep ocean into shallower waters, in which the incident long wave from the deep ocean is partially reflected at the shelf edge [10].

The model works by solving the shallow water equations, also known as the Saint Venant equations. Turbines can be included in the model by adding roughness terms at specific locations that extract energy from the flow. The methodology of Plew and Stevens [11] defines the total force induced by a tidal turbine on a flow through two components; the drag force caused by the support structures and the thrust force produced by the turbine rotors, giving:

$$F_{total} = F_D + F_T = \frac{1}{2}\rho A_S C_D \upsilon^2 + \frac{1}{2}\rho A_T C_T \upsilon^2 \tag{7}$$

The force at each node on the mesh in the area of the MCTA is then given by:

$$F_n \frac{F_{total}}{n} \tag{8}$$

Where F_n is the average force at each node in the array and n is the number of nodal points in the array area. The average kinetic power generated during a specified time period is then given by:

$$P_{ave} = \frac{1}{N}\sum_{i=1}^{N}\frac{1}{2}A_n C_P \rho \upsilon_i^3 \tag{9}$$

Where N is the number of time steps in the simulation.

Alternatively turbines can be modeled by defining a line discontinuity in water elevation, in which the water level downstream of a homogeneous row of turbines is related to the water level upstream. The depth change occurs across a row of turbines following mixing in the wake of the devices, which is assumed to happen over a sufficiently small distance that the change in depth occurs as a discontinuity across the line representing the row in the model [12].

Tidal constituents are defined at boundaries to drive the flow through the domain. These must contain the dominating principal diurnal, semi-diurnal and longer period constituents. Bathymetry data for the site must be obtained and mapped to the mesh. Consideration of mesh refinement in regions of rapidly changing geometry must be conducted to ensure that mesh independence is achieved.

Much work has been done in this area with different 2-D depth averaged numerical models. Examples of this are Blunden and Bahaj [2] who used Telemac-2D to model the flow effects of putting in tidal turbines at Portland Bill, UK. Karsten at al [13] used FVCOM to model the energy extraction in the Minas Passage, Bay of Fundy and Draper et al used ADCIRC to model the Pentland Firth [4].

Care must be taken when interpreting results from depth averaged models as there are limitations that must be considered. For example, depending on the vertical positioning of the turbines in the water column, it may not be the case that the depth-average flow velocity is what is being seen by the turbine in reality, due to the nature of the velocity profile. In addition, in a 2D model it is unlikely that flow profile changes due to the presence of the MCTA will be taken into account.

IV. EFFECT OF AN MCTA ON ITS SURROUNDINGS

Inevitably, deploying an MCTA in a tidal stream will cause changes to the flow in the vicinity. Examples of this are flow acceleration around an array and increased turbulence. The magnitude of these changes must be considered to evaluate what detrimental effects, if any, are caused by the presence of the MCTA. To do this, parameters such as the significant impact factor [2] have been established, defined as an acceptable proportion of kinetic energy flux through a channel that can be extracted without causing significant impact. Consideration into acceptable levels of sediment transport, navigational access and tidal exchange must also be made.

V. EFFECTS OF SEA BED ROUGHNESS

Sea bed roughness has a significant influence on the velocity profile of the flow. The region most heavily influenced is the roughness sublayer in the region closest to the sea bed. Its form is generally unknown [10]. This is problematic because turbines are likely to be placed in the roughness sublayer, so predicting the power they can generate becomes challenging because of the unpredictable nature of the flow velocity in this region.

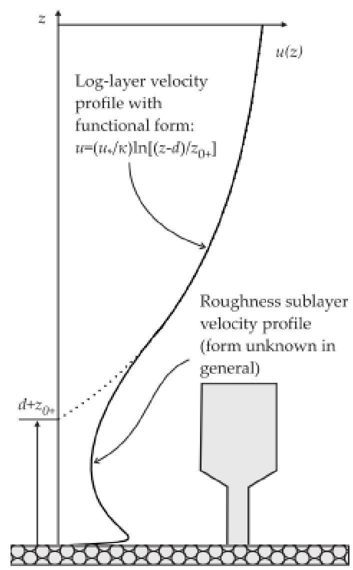

Fig. 2. Roughness sublayer profile [10]

Bed roughness also affects the turbulence kinetic energy, a feature that plays an important role in the wake recovery of a turbine. Turbulence kinetic energy in the wake region can enhance wake recovery by promoting mixing between the slow moving flow in the wake and the fast moving free stream around it. Experiments by Myers et al [6] show that turbulence kinetic energy generated from the seabed migrate up approximately 1/3rd of the total depth up the water column. It was found to be advantageous to position the turbines outside of this region because stagnation between the bottom of the turbine and the sea bed can occur, causing a reduction in shear motion due to reduced flow velocity. Positioning turbines in highly turbulent flow can also increase structural loading, reducing reliability.

It is likely that bed friction will vary spatially, directionally and temporally throughout any domain due to variation in local bathymetry, bed roughness, local depth etc. [4]. This makes modeling challenging as it requires the bed friction coefficient to vary spatially and temporally if the morphology of the bed changes, which is difficult to measure in reality. A sensitivity study conducted by Draper considers two cases where the bed friction coefficient is varied to cover all likely values at any given point in a numerical model. Two array configurations are considered: (i) a single row of low blockage turbines and (ii) four rows of highly blocked turbines. Available power is strongly dependent on sea bed friction for a small area of turbines, and less sensitive for larger scale developments. Regardless of this the results suggest it is important for the bed friction coefficient be determined as accurately as possible.

Sea bed roughness can be incorporated into 2-D depth averaged numerical models through definition of the Nikuradse equivalent sand roughness. k_s is dependent on size, spacing, pattern and variation of size of grain, however it only incorporates surface or skin friction caused by particles on the sea bed, and ignores form drag from ripples and/or dunes [14]. Commonly Manning's coefficient is used to characterize sea bed friction in engineering models, however it is an empirical relationship that does directly relate to the length scale of the roughness, which is why the Nikuradse coefficient has been used for this work.

VI. TELEMAC-2D NUMERICAL MODEL

Telemac-2D is a two dimensional depth averaged finite element software package used to model free-surface flows with the shallow water equations [15].

A. *Model Setup*

This work models a simple channel 15 km in length and 40 m deep. A long channel is used to capture the whole wake profile. The channel has slanting sides, with a bottom width of 600m and side wall slope of 5:1 (h:v). A mesh independence study concluded that a mesh with 50m edge length between nodes was sufficient to obtain a converged steady state solution without compromising on computational time. MCTAs are positioned in a 500 m x 500 m area with its center at (5000 m, 500 m) as shown in figure 3.

Liquid boundaries were defined at the east and west ends of the channel, with a head drop of 1 m from east to west to drive the flow in this direction. Solid boundaries were defined on the north and south boundaries. Friction from the channel bed and walls is defined through the Nikuradse coefficient, k_S=0.6 m. The model was run for a time period of 20 hours, with a time step of 5 seconds, which equates to 14400 time steps.

To calculate the force exerted by the turbines on the flow, a thrust coefficient, C_T=0.8, is used for current speeds between cut-in and rated power, as suggested by Bahaj et al [16]. It is important to note that as array density increases, the velocity profile will change, which can lead to a reduction in thrust coefficient.

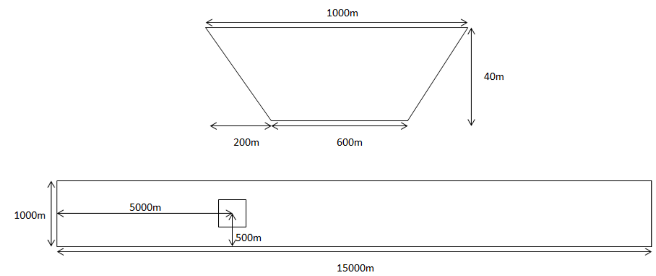

Fig. 3. Cross section and plan view of channel with the position of the 500 m x 500 m MCTA.

B. *Array Density*

Array density defines the number of turbines in a given area. Myers demonstrated experimentally using submerged actuator discs that for a single turbine, centerline velocity deficit can still be significant 10 diameters downstream and that downstream spacing between rows of turbines in an array could be 15-20 diameters [17]. A row spacing of 12.5 diameters is chosen for this work so that 3 rows can be fitted into the defined array area using 20 m diameter turbines. The number of turbines in each row defines the blockage ratio, ε, which is varied between 0.5 and 0.2, at 0.1 intervals, corresponding to 75 to 15 turbines in the array respectively, distributed evenly between the three rows.

C. *Sea Bed Roughness*

The effects of sea bed roughness are investigated by varying the Nikuradse friction coefficient between 0.3m and 1.5 m at 0.3 m intervals. This represents a roughness length of approximately 0.01 m and 0.05 m respectively. Both power and wake length are measured for varying sea bed roughness. Two array densities are investigated, 45 turbines (ε=0.3) and 75 turbines (ε=0.5).

VII. RESULTS AND DISCUSSION

A. Varying array density

Velocity plots show an increasing wake length as array density increases, as shown in figure 4.

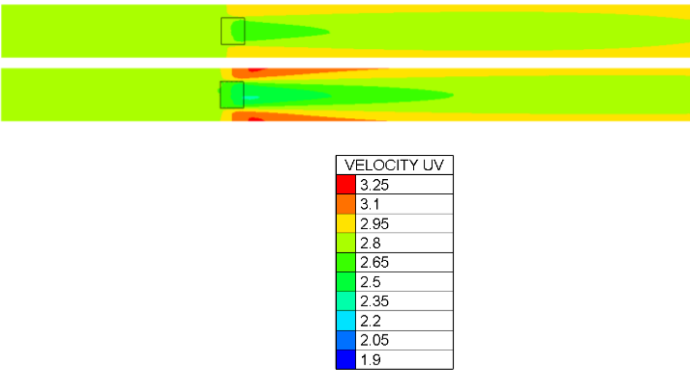

Fig. 4. Top: Array density = 0.038 (30 turbines, ε=0.3), Bottom: Array density = 0.094 (75 turbines, ε=0.5). Velocity in m/s.

This is to be expected, as increasing array density increases the force exerted on the flow by the turbines at the location of the array, causing it to decelerate in the array location. Flow accelerates around the array at the sides of the channel. Although out of the scope of this work, it is important to quantify this flow acceleration as it could have a detrimental effect on the channel in terms of sediment transport for example.

Wake length was measured for each array by finding the distance downstream of the array that flow velocity recovers to 95% of its original upstream magnitude. This measurement is taken at the centerline of the channel. Results are presented in figure 5. Wake length is non-dimensionalized by array width, A_w and non-dimensionalized array density is defined as total swept area of all turbines in the array, A_T divided by array plan area, A_a.

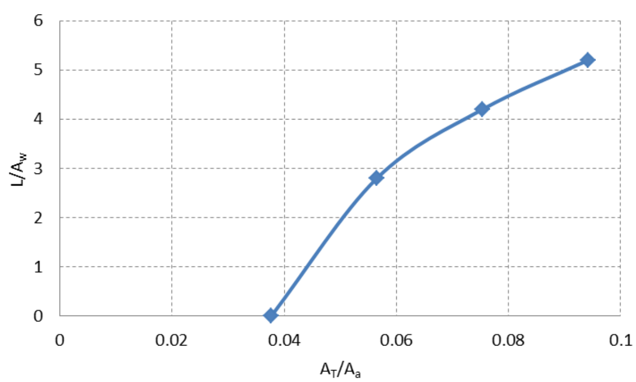

Fig 5. Variation in wake length for increasing array density.

For array density of 30 turbines (ε=0.3) or below, the wake length is negligible, because the force exerted on the flow distributed evenly between all nodes on the mesh in the array area is relatively small.

As the turbine density increases by increasing ε for each row, the force exerted on the flow by the turbines increases, at a rate proportional to the flow velocity squared multiplied by the total swept area of the turbines. At the maximum turbine density of 75 (ε=0.5), the wake propagates downstream to a distance 5 times the array depth, to 2500 m. The implications of this are of interest to developers, who need to know the severity of the wake formation throughout a spring-neap tidal cycle with respect to the placement of other MCTAs close to the one in question.

Power is calculated using equation 7 to understand how it scales with array density and blockage ratio. As would be expected, increasing turbine density increases total power generation because increasing the number of devices allows a greater proportion of the resource to be captured. This effect is replicated in the numerical model by a higher average force exerted on the flow at each node in the array. Figure 6 gives a comparison between numerical results and the Lanchester-Betz limit commonly used for wind turbines, given in equation 4. It can be seen that results compare well for a 15 turbine array, but as the array density is increased, the rate of power generation increases dramatically in comparison to a modest linear increase from the numerical results. This is because the Lanchester-Betz limit becomes less valid for high density arrays when the blockage ratio is high and the geometrical constraints of the channel relative to the array dimensions have a significant effect on the flow behavior. Power, P is non-dimensionalized by the power of a single turbine operating in the channel with C_p=0.45, P_0.

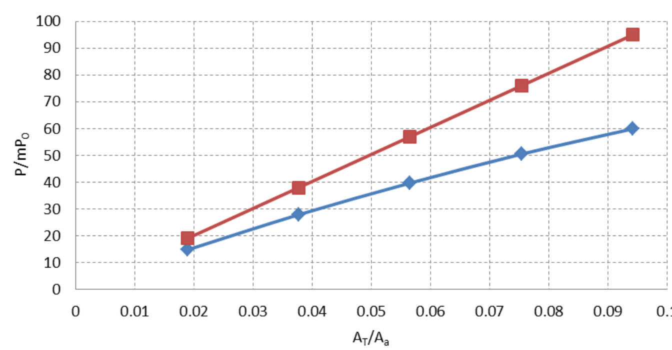

Fig. 6. Power generated by MCTAs of varying array density. Diamond pointers: Telemac result, square pointers: $P_{max}=8/27\rho A u^3$ (Equation 4).

The numerical results indicate that as turbines are added to each row of the array to increase turbine density and blockage ratio, power generated by the array increases linearly. This seems encouraging and suggests that adding turbines is beneficial as there is an increase in power that is directly proportional to array density. However closer inspection of the average power produced by each turbine (which assumes the total power generated by the array is distributed evenly across all turbines) shows a decrease occurs when adding more turbines, as seen in figure 7. Here m is the total number of turbines in the array.

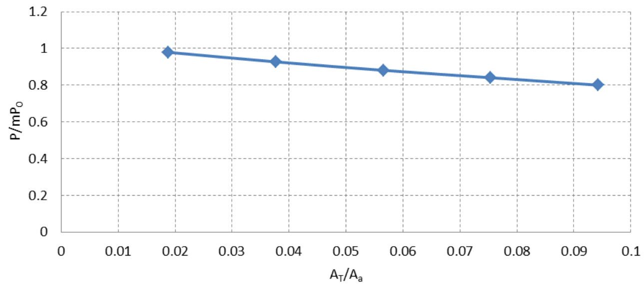

Fig. 7. Average power produced per turbine for increasing array density.

Increasing turbine density reduces the power per turbine in the array. By considering the relationship between power, flow velocity and turbine swept area given in equation 1, this result indicates that when array density is increased, the reduction in flow velocity dominates the increase in total turbine area, leading to diminishing returns for total power generation in this case.

It is important to note that in reality turbines in an array will not each produce the same amount of power at any given point in time. Turbines in the rows downstream of the front of an array are likely to suffer from receiving a lower flow velocity due to the wakes formed by turbines in the rows upstream. Vennell suggests that the approach to array optimization should be to maximize the blockage ratio of the first row of turbines, then add in additional rows with consideration to the flow effects caused by the first row [18]. This may minimize row interaction, but could be detrimental to wake length.

B. *Varying seabed roughness*

Velocity plots show a decreasing wake length as sea bed roughness is increased at high blockage ratio, but a minimal effect at low blockage ratio, as shown in figures 8, 9 and 10.

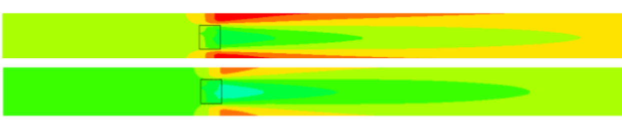

Fig. 8. Wake profiles, top: blockage = 0.5, ks = 0.3
bottom: blockage = 0.5, ks = 1.2, Velocity scale as in figure 4.

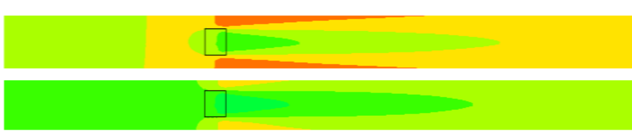

Fig. 9. Wake profiles, top: blockage = 0.3, ks = 0.3
bottom: blockage = 0.3, ks = 1.2, Velocity scale as in figure 4.

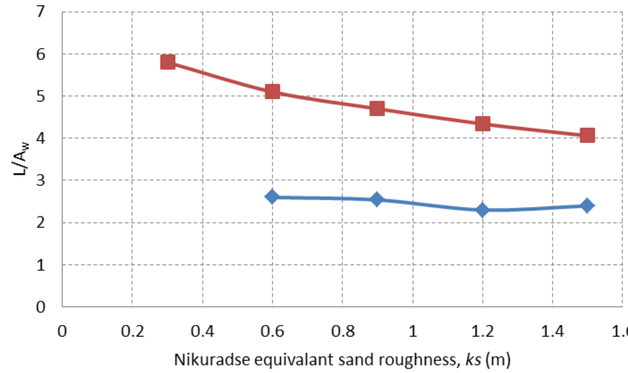

Fig. 10. Wake length for varying seabed roughness at two array density of 0.057 (45 turbines) - diamond pointers and 0.094 (75 turbines) - square pointers.

Low seabed friction gives a higher inlet flow velocity, as can be seen in figures 8 and 9. This higher flow velocity propagates up the channel, meaning the flow velocity seen by the MCTA is also higher. The drag force created by the array, F_{drag} is proportional to the flow velocity, u^2, so the drag created by the MCTA is greatest at low seabed roughness and the wake generated propagates further downstream.

Equation 5 states that the components of energy extraction can be broken down into three components; seabed friction, drag from support structures and power for energy extraction. At low seabed friction, the drag from the MCTA takes a higher proportion of the total drag in the channel. Conversely, at high bed friction, the drag from the MCTA takes a lower proportion of the total drag in the channel meaning the drag caused by the MCTA does not have such a dominating effect. This is true also when increasing the turbine density, as a higher density array means a higher proportion of the total energy extracted from the flow is from the drag created by the turbines. This could be why there is a greater dependence on seabed roughness for higher density arrays with respect to wake length.

Results show that for an array containing 45 turbines (ε=0.3), power decreases with increased roughness. A possible reason for this is that increased sea bed roughness increases shearing of the flow, especially in the roughness sublayer as discussed in section V. This reduces the depth averaged velocity, as seen at the inlet in figures 5 and 6.

Vennell stated that due to bottom friction, shallow channels are already highly stressed, hence increasing the total drag in the channel, defined by λ_{total} in equation 4 by adding tidal turbines results in diminishing returns. This can be seen in figure 11, where increasing sea bed friction results in a reduction in the power generated by a 45 turbine array (ε=0.3).

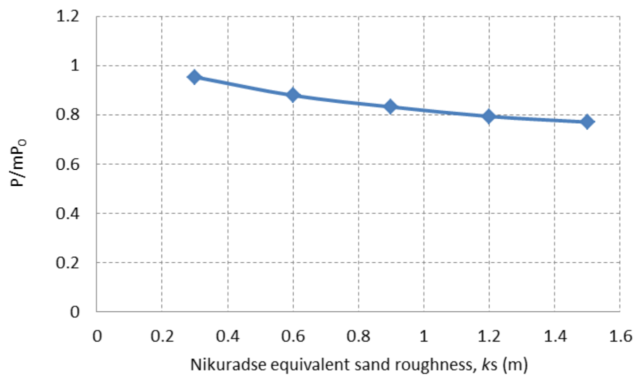

Fig. 11. Average power generated per turbine in a MCTA containing 45 turbines for increasing roughness length.

VIII. CONCLUSIONS

Results from a Telemac-2D model with a simple channel flow show the effects of array density and sea bed roughness on the wake recovery and power generation of MCTAs set out in a geometry of 500 m x 500 m. Wake length becomes significant when more than 30 turbines are used in the array, corresponding to a blockage ratio greater than 0.3. It is seen that increasing array density up to 75 turbines increases overall power generation, however there is a diminishing return on the average power produced by each turbine.

The effects of seabed roughness are investigated through variation in the Nikuradse coefficient, k_s, and it is shown that increasing the seabed roughness within a very rough range of values decreases the wake length and power generation, most likely due to a reduced depth averaged flow velocity at the inlet to the channel. Results suggest that high density arrays are more sensitive to seabed roughness with respect to wake length.

Detail must be added to the model for it to replicate the dynamics of a real tidal channel. Consideration of tidal constituents defined at the liquid boundaries to simulate the variation in flow velocity that occurs over a spring-neap tidal cycle will allow analysis over a longer time period. It is intended to incorporate turbine cut-in and cut-out flow velocities to allow the turbines to be responsive to the unsteady conditions set by the tidal constituents over a tidal cycle. Drag from the support structures of the turbine devices is believed to be significant, so when more knowledge on the drag associated with the profile of the structure is gained, this will be incorporated into the model. Once this detail is added comparison will be made with a real tidal channel also modeled using Telemac-2D.

REFERENCES

[1] D. Pugh, "Tides, Surges and Mean Sea-Level.", 1987.

[2] L. Blunden and A. Bahaj, "Tidal energy resource assessment for tidal stream generators," *… , Part A: Journal of Power and Energy*, 2007.

[3] C. Garrett and P. Cummins, "The power potential of tidal currents in channels," *… of the Royal Society A: …*, 2005.

[4] T. A. A. Adcock, S. Draper, G. T. Houlsby, A. G. L. Borthwick, and S. Serhadlıoğlu, "The available power from tidal stream turbines in the Pentland Firth," 2013.

[5] H. E. Seim and C. R. Edwards, "Comparison of Buoy-Mounted and Bottom-Moored ADCP Performance at Gray's Reef," *Journal of Atmospheric and Oceanic Technology*, vol. 24, no. 2, pp. 270–284, Feb. 2007.

[6] L. E. Myers and a. S. Bahaj, "Experimental analysis of the flow field around horizontal axis tidal turbines by use of scale mesh disk rotor simulators," *Ocean Engineering*, vol. 37, no. 2–3, pp. 218–227, Feb. 2010.

[7] G. Sutherland, M. Foreman, and C. Garrett, "Tidal current energy assessment for Johnstone Strait, Vancouver Island," *Proceedings of the Institution of Mechanical Engineers, Part A: Journal of Power and Energy*, vol. 221, no. 2, pp. 147–157, Jan. 2007.

[8] C. Garrett and P. Cummins, "The efficiency of a turbine in a tidal channel," *Journal of Fluid Mechanics*, vol. 588, pp. 243–251, Sep. 2007.

[9] R. Vennell, "The energetics of large tidal turbine arrays," *Renewable Energy*, 2012.

[10] L. Blunden, "ePrints Soton New Approach to tidal stream energy analysis at sites in the English Channel," 2007

[11] D. R. Plew and C. L. Stevens, "Numerical modelling of the effect of turbines on currents in a tidal channel – Tory Channel, New Zealand," *Renewable Energy*, vol. 57, pp. 269–282, Sep. 2013.

[12] S. Draper, G. T. Houlsby, M. L. G. Oldfield, and A. G. L. Borthwick, "Modelling Tidal Energy Extraction in a Depth-Averaged Coastal Domain," pp. 1045–1052, 2009.

[13] R. H. Karsten, J. M. McMillan, M. J. Lickley, and R. D. Haynes, "Assessment of tidal current energy in the Minas Passage, Bay of Fundy," *Proceedings of the Institution of Mechanical Engineers, Part A: Journal of Power and Energy*, vol. 222, no. 5, pp. 493–507, Aug. 2008.

[14] M. J. Marriott and R. Jayaratne, "HYDRAULIC ROUGHNESS - LINKS BETWEEN MANNING ' S COEFFICIENT , NIKURADSE ' S EQUIVALENT SAND ROUGHNESS AND BED GRAIN SIZE," pp. 27–32, 2010.

[15] Jean-Michel Hervouet, *Hydrodynamics of free surface flows modelling with the finite element method*. 2007.

[16] A. S. Bahaj, a. F. Molland, J. R. Chaplin, and W. M. J. Batten, "Power and thrust measurements of marine current turbines under various hydrodynamic flow conditions in a cavitation tunnel and a towing tank," *Renewable Energy*, vol. 32, no. 3, pp. 407–426, Mar. 2007.

[17] L. E. Myers, a. S. Bahaj, R. I. Rawlinson-Smith, and M. Thomson, "The Effect of Boundary Proximity Upon the Wake Structure of Horizontal Axis Marine Current Turbines," *Volume 6: Nick Newman Symposium on Marine Hydrodynamics; Yoshida and Maeda Special Symposium on Ocean Space Utilization; Special Symposium on Offshore Renewable Energy*, pp. 709–719, 2008.

[18] R. Vennell, "Tuning tidal turbines in-concert to maximise farm efficiency," *Journal of Fluid Mechanics*, 2010.